Phosphatidylethanolamine Modulates Ca-ATPase Function and Dynamics†

Gregory W. Hunter, Sewite Negash, and Thomas C. Squier*

Biochemistry and Biophysics Section, Department of Molecular Biosciences, University of Kansas, Lawrence, Kansas 66045-2106

Received September 15, 1998; Revised Manuscript Received November 25, 1998

ABSTRACT: Phospholipids containing phosphoethanolamine (PE) headgroups within biological membranes have been suggested to be important with respect to the functional regulation of membrane proteins, including the Ca-ATPase in sarcoplasmic reticulum (SR). To investigate the role of PE headgroups in modulating the catalytic activity of the Ca-ATPase, we have reconstituted the Ca-ATPase into unilamellar liposomes containing defined amounts of dioleoylphosphatidylethanolamine (DOPE) and dioleoylphosphatidylcholine (DOPC). The enzymatic activity of the Ca-ATPase progressively increases upon incorporation of increasing amounts of PE into reconstituted vesicles, and approaches that characteristic of native SR membranes. To identify structural changes that correlate with enzyme activation, we have used frequency-domain phosphorescence spectroscopy to measure the rotational dynamics of erythrosin isothiocyanate covalently bound to Lys_{464} in the phosphorylation domain of the Ca-ATPase. Progressive increases in the rotational dynamics of the phosphorylation domain result from the incorporation of increasing amounts of DOPE, and correlate with enhanced enzymatic function. These results suggest that PE headgroups induce dynamic structural rearrangements involving the phosphorylation domain that modify the rates of nucleotide utilization. In contrast, no changes in the rotational dynamics of the lipid acyl chains are observed irrespective of the PE content. Therefore, the enhanced ATP hydrolytic activity associated with the incorporation of DOPE into these proteoliposomes is the result of specific noncovalent interactions involving PE phospholipid headgroups and the Ca-ATPase.

The phospholipid composition in different cellular organelles is tightly regulated, and alterations in specific membrane lipids have been observed to correlate with a range of pathological conditions that may involve alterations in the catalytic activity of many different membrane proteins (*1*−*3*). Active transport proteins have been suggested to be particularly sensitive to alterations in lipid composition, since during ion transport these proteins have been shown to undergo large volume changes (*4*−*7*). Consistent with an important functional role for membrane phospholipids in regulating membrane protein function, the catalytic activity of the Ca-ATPase in skeletal sarcoplasmic reticulum (SR)[1] membranes has previously been suggested to be modulated by the phosphatidylethanolamine (PE) content of the membrane (*8*−*11*). However, earlier reconstituted preparations exhibited minimal catalytic activity. Thus, differences in the extent of calcium accumulation within the lumen of vesicles containing variable amounts of PE could have been the result of other physical factors that may involve, for example, differences in the stability of the Ca-ATPase or rates of calcium efflux from the vesicles. Critical to understanding the regulation of Ca-ATPase function by the PE content in the membrane is the reconstitution of a fully functional Ca-ATPase into homogeneous unilamellar vesicles with a defined phospholipid composition, permitting the differentiation between the influence of alterations in phospholipid composition from other physical constraints that also may modulate calcium accumulation. We have, therefore, measured catalytic activity following the asymmetrical reconstitution of the Ca-ATPase into tightly sealed proteoliposomes containing variable amounts of dioleoyl-PE (DOPE). To investigate possible changes in the structure or dynamics of the Ca-ATPase that may correlate with changes in the PE content of the bilayer, we have used frequency-domain phosphorescence spectroscopy to investigate the dynamic structure of the Ca-ATPase specifically modified at Lys_{464} within the phosphorylation domain with the long-lived phosphorescent probe erythrosin isothiocyanate (Er-ITC) (*12*). Complementary fluorescence anisotropy measurements of phospholipid acyl chain dynamics used the phospholipid analogue 1-(4-trimethylammoniumphenyl)-6-phenyl-1,3,5-hexatriene (TMA-DPH) partitioned into reconstituted proteoliposomes, and indicate that PE does not alter phospholipid acyl chain dynamics. Correlations between the maximal ATP hydrolytic activities of the Ca-ATPase and the dynamic structure of the phosphorylation domain suggest that PE

† Supported by the National Institutes of Health (Grant GM46837).

* Correspondence should be addressed to this author. Telephone: (913)-864-4008. FAX: (913)-864-5321. E-mail: TCSQUIER@KUHUB.CC.UKANS.EDU.

[1] Abbreviations: ATP, adenosine 5′-triphosphate; BSA, bovine serum albumin; CCCP, carbonyl cyanide 3-chlorophenylhydrazone; $C_{12}E_9$, polyoxyethylene 9 lauryl ether; DOPE, dioleoylphosphatidylethanolamine; DOPC, dioleoylphosphatidylcholine; EGTA, ethylene glycol bis-(β-aminoethyl ether)-*N*,*N*,*N*′,*N*′-tetraacetic acid; Er-ITC, erythrosin 5-isothiocyanate; FURA-2,1-[2-(5-carboxyazol-2-yl)-6-aminobenzofuran-5-oxyl]-2-(2-amino-5-methylphenoxy)ethane-*N*,*N*,*N*′,*N*′-tetraacetic acid; MOPS, 3-(*N*-morpholino)propanesulfonic acid; PC, phosphatidylcholine; PE, phosphatidylethanolamine; r_o, initial anisotropy; r_∞, residual anisotropy; *S*, order parameter; SR, sarcoplasmic reticulum; TMA-DPH, 1-(4-trimethylammoniumphenyl)-6-phenyl-1,3,5-hexatriene; $\langle\tau\rangle$, average fluorescence lifetime; ϕ, rotational correlation time.

10.1021/bi9822224 CCC: $18.00
Published on Web 01/09/1999

headgroups enhance the catalytic activity of the Ca-ATPase through specific PE phospholipid headgroup interactions that modulate the dynamic structure of the Ca-ATPase.

EXPERIMENTAL PROCEDURES

Materials. KCl was purchased from Research Organics (Cleveland, OH). Sucrose, TRIS (free base), and MOPS [3-(*N*-morpholino)propanesulfonic acid] were obtained from Fisher Scientific (Pittsburgh, PA). $CaCl_2$ standard solution was from VWR (St. Louis, MO). A23187, ammonium molybdate, ATP (disodium salt), isomer II of Er-ITC (erythrosin 5-isothiocyanate), EGTA, β-D(+)-glucose, $MgCl_2$, polyoxyethylene 9 lauryl ether ($C_{12}E_9$), and sulforhodamine B (Texas Red) were from Sigma (St. Louis, MO). BSA, glucose oxidase, and catalase were from Worthington (Freehold, NJ). The proton ionophore carbonyl cyanide 3-chlorophenylhydrazone (CCCP) was obtained from Fluka Chemical Corp. (Ronkonkoma, NY). All phospholipids and 2-[3-(diphenylhexatrienyl)propanoyl]-1-hexadecanoyl-*sn*-glycero-3-phosphocholine (TMA-DPH) were obtained from Avanti Polar Lipids (Alabaster, AL). 1-[2-(5-Carboxyazol-2-yl)-6-aminobenzofuran-5-oxyl]-2-(2-amino-5-methylphenoxy)ethane-*N*,*N*,*N*′,*N*′-tetraacetic acid (FURA-2) was purchased from Molecular Probes, Inc. (Eugene, OR). Bio-Beads SM-2 were purchased from Bio-Rad (Richmond, CA). SR membranes were isolated from rabbit fast-twitch skeletal muscle, essentially as previously described (*13*). SR lipids were extracted as previously described (*14*, *15*). All samples were stored in 20 mM MOPS (pH 7.0) and 0.3 M sucrose at −70 °C.

Purification and Reconstitution of Ca-ATPase. Native SR membranes (8 mg mL^{-1}) in 50 mM MOPS (pH 7.0), 1 mM $MgCl_2$, 1 mM $CaCl_2$, and 0.6 M sucrose were solubilized in 35 mM $C_{12}E_9$. Following removal of nonsolubilized membranes by ultracentrifugation (100000*g* for 45 min), the Ca-ATPase was purified using a Reactive Red 120 affinity column, essentially as previously described (*16*, *17*). Following extensive elution of nonspecifically bound protein from the column [50 mM MOPS (pH 7.0), 9 mM $C_{12}E_9$, 1 mM $MgCl_2$, 1 mM $CaCl_2$, and 0.3 M sucrose], the purified Ca-ATPase was eluted upon addition of 0.8 mM ADP (Figure 1). Approximately 24 membrane phospholipids remain associated with each Ca-ATPase following purification. The purified Ca-ATPase was then mixed with an equal mass of phospholipids (4 mg mL^{-1}) suspended in 40 mM octyl glucopyranoside. In all cases, 10 mol % egg phosphatidic acid (PA) was included to prevent vesicle aggregation (*18*). Detergent was slowly removed through the addition of Bio-Beads (80 mg mL^{-1}), essentially as previously described (*18*, *19*). Following 1 h increments at 25 °C, two additional aliquots of Bio-Beads were added, and the reconstituted vesicles were sedimented at 100000*g* (45 min).

Enzymatic Activity Assays. Protein concentrations were measured using the Amidoschwarz protein assay using nitrocellulose paper and Amidoblack stain (*20*). Phospholipid content was measured using a protocol for the detection of liberated phospholipid phosphate, as previously described (*21*). Calcium-dependent rates of ATP hydrolysis were measured as an ammonium molybdate complex of phosphate at 25 °C (*22*), and involved 0.05 mg mL^{-1} SR vesicles in a medium containing 25 mM MOPS (pH 7.0), 100 mM KCl, 5 mM $MgCl_2$, 5 mM ATP, 6 μM A23187, 0.5 μM CCCP, 2 mM EGTA, and sufficient calcium to yield the indicated free calcium concentration. Free calcium concentrations were directly measured using FURA-2, whose dissociation constant for calcium under these conditions was measured to be 186 ± 3 nM (*23*). The calcium-dependent activation of the Ca-ATPase was fit to a model involving the cooperative binding of two ligands:

$$\text{ATPase Activity} = \frac{K_1[Ca^{2+}]_{free} + 2K_2[Ca^{2+}]^2_{free}}{2(1 + K_1[Ca^{2+}]_{free} + K_2[Ca^{2+}]^2_{free})} \quad (1)$$

where K_1 is the macroscopic equilibrium constant, and corresponds to the sum of the intrinsic equilibrium constants (k_1 and k_2) associated with calcium activation of the Ca-ATPase; and K_2 is the intrinsic equilibrium constant for calcium activation and corresponds to the product of equilibrium constants ($k_1k_2k_c$) (*24*). This assessment of calcium activation permits a determination of the cooperativity (i.e., k_c) between high-affinity calcium binding sites on the Ca-ATPase.

Physical Characteristics of Reconstituted Vesicles. The average diameter of the reconstituted vesicles containing the Ca-ATPase was measured using dynamic light scattering (Nicomp 370; Santa Barbara, CA), and the distribution of vesicle sizes was fit to a Gaussian distribution (*25*).

Fluorescence Measurements. Excitation of TMA-DPH involved the 364 nm line from a Coherent Innova 400 argon ion laser (Santa Clara, CA), and the fluorescence emission was detected after a Schott GG400 long-pass filter using an ISS K2 frequency domain fluorometer, as described previously (*26*). Excitation of FURA-2 was at 345 nm, and emission was monitored at 510 nm using a Spex FluoroMax-2 (Edison, NJ).

Phosphorescence Measurements. Er-ITC was covalently bound to Lys_{464} on the Ca-ATPase at a stoichiometry of approximately 0.2 mol of Er-ITC bound per mole of Ca-ATPase, essentially as previously described (*12*). Frequency-domain phosphorescence data were collected using an ISS-K2 fluorometer equipped with a low-frequency modulator. Er-ITC-derivatized SR vesicles (0.3 mg/mL) were excited using approximately 1 mW of 514 nm modulated light from an argon ion laser (Coherent Corp., Palo Alto, CA), and the phosphorescence emission was collected after a Schott RG697 long-pass filter essentially as previously described (*27*). Prior to the measurement of phosphorescence, the concentration of dissolved oxygen in a 3 mL sealed cuvette was reduced enzymatically by the addition of 17 mM glucose, 3 units of glucose oxidase activity, and 30 units of catalase activity, and subsequent incubation in the dark for at least 5 min (*28*).

Data Analysis. Fluorescence or phosphorescence intensity decays [i.e., $I(t)$] were fit using the Globals software package (University of Illinois, Urbana−Champaign) to a sum of exponentials:

$$I(t) = \sum_{i=1}^{n} \alpha_i e^{(-t/\tau_i)} \quad (2)$$

where α_i are the preexponential factors, τ_i are the excited

state lifetime decay times, and n is the number of exponential components required to describe the decay. Unless otherwise indicated, data were analyzed using frequency-independent errors in the phase and modulation that were assumed to be 0.2° and 0.01, respectively. After the measurement of the intensity decay, one typically calculates the average lifetime, $\langle\tau\rangle$, which is weighted by the fractional intensities (f_i) associated with each of the preexponential terms, where

$$\langle\tau\rangle \equiv \frac{\sum_i \alpha_i \tau_i^2}{\sum_i \alpha_i \tau_i} = \sum_i f_i \tau_i \quad (3)$$

and $\langle\tau\rangle$ is directly related to the average time the fluorophore is in the excited state. The frequency-domain anisotropy decays [i.e., $r(t)$] were fit to a model involving a sum of exponentials and a residual anisotropy (r_∞), where

$$r(t) = (r_o - r_\infty)\sum_i^n g_i e^{-t/\phi_i} + r_\infty \quad (4)$$

r_o is the limiting anisotropy in the absence of rotational diffusion, ϕ_i are the rotational correlation times, and $r_o \times g_i$ are the preexponential terms relating to the amplitudes of the total anisotropy loss associated with each correlation time. Additional details are described elsewhere (*27*, *29*, *30*). In all cases, parameter values are determined by minimizing the χ_R^2 (the F statistic) which serves as a goodness-of-fit parameter that provides a quantitative comparison of the adequacy of different assumed models (*31*, *32*). In the cases of the DPH analogues, which have an axis of symmetry relative to the membrane normal, the order parameter (S) associated with the phospholipid acyl chains was calculated from the measured residual anisotropy (*26*), where

$$S = \left(\frac{r_\infty}{r_o}\right)^{0.5} \quad (5)$$

RESULTS

Purification and Reconstitution of the Ca-ATPase. The Ca-ATPase was purified to homogeneity using a Reactive Red 120 affinity column (Figure 1), and was subsequently reconstituted with variable amounts of DOPC and DOPE, as previously described (*16*−*18*). Irrespective of the amount of PE in the membrane, the average diameters of reconstituted vesicles were 90 ± 7 nm, and the average lipid-to-protein ratio of these reconstituted preparations was determined to be 135 ± 24 mol of phospholipid per mole of Ca-ATPase. The reconstituted vesicles are tightly sealed, in all cases exhibiting a greater than 2-fold increase in steady-state rates of ATP hydrolysis upon elimination of calcium gradients across the lumen through the addition of the calcium ionophore A23187 and the proton ionophore CCCP (data not shown). Furthermore, following vesicle solubilization in the presence of 9 mM $C_{12}E_9$, the rates of ATP hydrolysis are virtually identical to that of the Ca-ATPase in native SR upon correction for differences in protein abundance (data not shown). To determine the asymmetry of Ca-ATPase incorporation, the cytosolic portion of the Ca-ATPase in native SR membranes was covalently modified with 5-iodoacetamidofluorescein (IAF), essentially as previously described (*33*). Following reconstitution, greater than

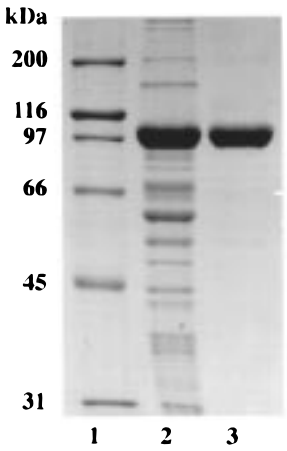

FIGURE 1: Affinity purification of the Ca-ATPase. SDS−PAGE of 10 μg of native SR membranes (lane 2) or 4 μg of the Ca-ATPase following affinity purification using a Reactive Red 120 affinity column (lane 3) (*81*). Molecular mass standards (lane 1) correspond to bovine carbonic anhydrase (31 kDa), hen egg white ovalbumin (45 kDa), bovine serum albumin (66 kDa), rabbit muscle phosphorylase B (97 kDa), *E. coli* β-galactosidase (116 kDa), and rabbit skeletal muscle myosin (200 kDa).

95% of the IAF chromophore was released into the supernatant following tryptic digestion, irrespective of the PE content of the membrane. Thus, the uniformity of these reconstituted vesicles with respect to vesicle size, enzyme stability, or asymmetry ensures that PE-dependent differences in catalytic activity (see below) are not the result of trivial effects.

Relationship between PE Content and Enzymatic Activity. Maximal rates of ATP hydrolytic activity increase about 2-fold when the Ca-ATPase is reconstituted in the presence of increasing amounts of DOPE, and approach that associated with native SR membranes upon correcting for differences in the relative abundances of the Ca-ATPase in the reconstituted and native membranes (Figure 2). The addition of the calcium ionophore A23187 and the protonophore CCCP prior to measuring enzyme activity ensures that the PE-dependent activation of the Ca-ATPase is not the result of trivial effects relating to possible differences in membrane permeability. The free energies associated with calcium binding and activation of the Ca-ATPase reconstituted into vesicles with variable amounts of PE are similar to those associated with native SR; no significant differences in cooperative interactions between the high-affinity calcium binding sites result from differences in PE concentration (Table 1). These latter results indicate that the PE-dependent enhancement of ATPase activity involves the facilitation of subsequent steps in the reaction cycle involving nucleotide utilization and phosphoenzyme hydrolysis.

Phosphorescence Lifetime and Anisotropy Measurements. Erythrosin isothiocyanate (Er-ITC) selectively modifies Lys_{464} within the phosphorylation domain of the Ca-ATPase, without interfering with the catalytic activity associated with the high-affinity nucleotide binding site (*12*). Thus, this probe provides a tool for monitoring dynamic structural changes of the phosphorylation domain that may correlate with PE-induced enzyme activation. Measurements of protein dynamics require independent measurements of the phosphorescence lifetimes. We have therefore measured the phase delay and modulation of Er-ITC bound to the Ca-ATPase at 23

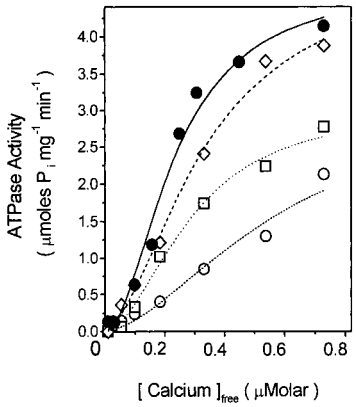

FIGURE 2: PE-dependent modulation of ATP hydrolytic activity. Samples correspond to either native SR membranes (●) or the Ca-ATPase reconstituted in the presence of 0% PE (○), 25% PE (□), and 50% PE (◇). Calcium-dependent rates of ATP hydrolysis were measured at 25 °C in the presence of 20 mM MOPS (pH 7.0), 0.1 M KCl, 5 mM $MgCl_2$, 5 mM ATP, 2 mM EGTA, 6 μM A23187, 0.5 μM CCCP, and sufficient $CaCl_2$ to yield the indicated free calcium concentrations, which were directly measured using FURA-2, which has a binding affinity of 186 ± 3 nM under these experimental conditions (*23*). Values for reconstituted samples represent the average of two independent determinations, and average errors were 11% of the indicated values. Values for native SR membranes (●) are taken from reference (*82*), and were corrected for the relative abundance of the Ca-ATPase.

Table 1: Free Energy Changes Associated with Calcium Activation of the Ca-ATPase in Native and Reconstituted Membranes[a]

sample	ΔG_1 (kcal mol^{-1} K^{-1})	ΔG_2 (kcal mol^{-1} K^{-1})	ΔG_c (kcal mol^{-1} K^{-1})	V_{max} (μmol of P_i mg^{-1} min^{-1})
native SR	−8.4 ± 0.2	−18.1 ± 0.1	−2.1 ± 0.2	4.4 ± 0.2[b]
reconstituted SR				
0% PE	−7.7 ± 0.6	−17.0 ± 0.4[c]	−2.5 ± 0.2 [c]	2.3 ± 0.3
25% PE	−8.1 ± 0.3	−17.8 ± 0.2	−3.4 ± 0.8	2.8 ± 0.2
50% PE	−8.4 ± 0.2	−17.7± 0.2	−2.2 ± 0.3	3.9 ± 0.2

[a] Data in Figure 1 were fit using eq 1 to estimate binding energies, cooperativity, and maximal ATPase activity (V_{max}) associated with calcium activation of the Ca-ATPase. [b] Maximal ATPase activity is expressed in terms of ATP hydrolytic activity per milligram of Ca-ATPase, which corresponds to 4.6 ± 0.2 nmol of Ca-ATPase/mg of SR protein (*12*, *79*). [c] Observed differences in binding energies relative to native SR (top line) were judged statistically significant using the Student's *t*-test ($P < 0.05$). Errors were propagated (*80*).

frequencies between 0.1 and 100 kHz (Figure 3). The intensity decay of Er-ITC bound to the Ca-ATPase can be adequately described as a sum of four exponentials, as shown by the essentially random distribution of weighted residuals (Figure 3C). There are, however, small systematic errors in the residuals associated with the modulation data upon fitting the data to a sum of four exponentials, which are not improved upon inclusion of additional fitting parameters. The four individual lifetime components and corresponding fractional intensities are independent of the PE content of the membrane (Figure 4), indicating that the environment surrounding the Er-ITC probe is unaltered by the PE content of the membrane. The average phosphorescence lifetime ($\langle\tau\rangle$) is 157 ± 8 μs, which is sufficiently long to permit the measurement of internal domain motions and the overall rotational motion of the Ca-ATPase with respect to the membrane normal (*27*).

Resolution of the rotational dynamics of Er-ITC bound to the Ca-ATPase involved the measurement of the differential

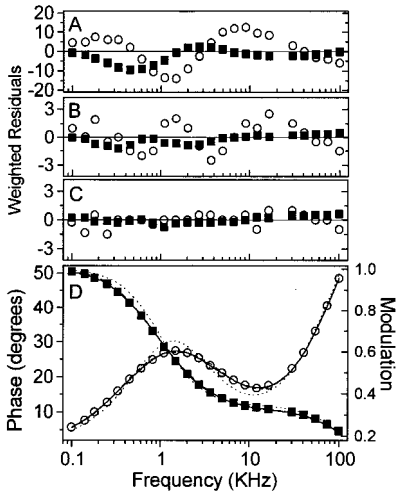

FIGURE 3: Phosphorescence lifetime data. Frequency−response and multiexponential fits to the data corresponding to the phase shift (○) and modulation (■) for Er-ITC bound to Lys_{464} in the Ca-ATPase following reconstitution into proteoliposomes (D). Weighted residuals corresponding to the nonlinear least-squares fit to a multiexponential decay corresponding to (A) two-, (B) three-, and (C) four-exponential fits to the data are shown, whose respective χ^2_R values are 34, 1.3, and 0.2. The corresponding two- (dotted line), three- (dashed line), and four- (solid line) exponential fits to the data are shown in panel D. The weighted residuals correspond to the difference between the experimental data and the calculated fit divided by the standard error the individual measurements, which was assumed to be 0.2° and 0.01 for the phase and modulation data, respectively. Lifetime measurements involved 0.3 mg mL^{-1} Ca-ATPase in 20 mM MOPS (pH 7.0) at 25 °C.

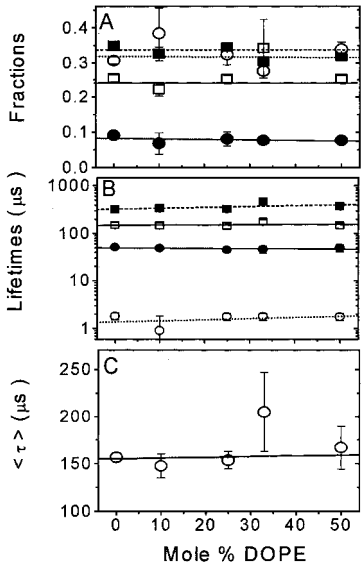

FIGURE 4: Phosphorescence lifetime parameters. Fractional intensities (A), associated lifetime components (B), and calculated average lifetimes (C) for the Ca-ATPase reconstituted in the presence of varying amounts of PE. Average lifetimes are calculated as $\langle\tau\rangle = \Sigma f_i\tau_i$, where $f_i = \alpha_i\tau_i/\Sigma\alpha_i\tau_i$. Average values and standard errors of the mean are shown for three separate measurements. Experimental conditions are as described in the legend to Figure 3.

phase and modulated anisotropy between 0.1 and 20 kHz (Figure 5). The frequency-domain anisotropy data can be adequately described as a sum of two exponentials and a residual anisotropy, as shown by the randomly weighted residuals (Figure 5C). The measured rotational correlation times have previously been shown to correspond to the domain motion of the phosphorylation domain ($\phi_1 \approx 6$ μs)

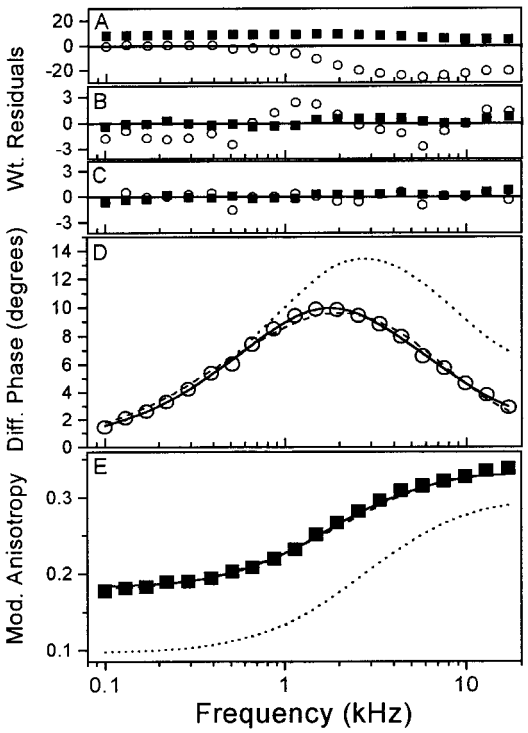

FIGURE 5: Phosphorescence anisotropy data. Differential phase (○; panel D) and modulated anisotropy (■; panel E) data and corresponding multiexponential fits to models involving a single exponential (dotted line; A), two exponentials (dashed line; B), and two exponentials and a residual anisotropy (solid line; C), whose respective χ^2_R values are 204, 1.4, and 0.3. Frequency-independent errors were assumed to be 0.2° and 0.01 for the differential phase and modulated anisotropy, respectively. Experimental conditions are as indicated in the legend to Figure 3.

Table 2: Rotational Dynamics of Er-ITC-Labeled Ca-ATPase[a]

sample	r_o	g_1	ϕ_1 (μs)	g_2	ϕ_2 (μs)	r_∞
native SR[b]	0.37	0.61	5	0.21	50	0.07
	(0.03)	(0.04)	(1)	(0.03)	(10)	(0.02)
reconstituted SR						
0% PE	0.35	0.41	6	0.35	130	0.09
	(0.01)	(0.05)	(1)	(0.04)	(20)	(0.01)
10% PE	0.35	0.44	6	0.29	220	0.06
	(0.01)	(0.06)	(1)	(0.11)	(20)	(0.01)
25% PE	0.35	0.50	6	0.30	160	0.07
	(0.01)	(0.08)	(1)	(0.08)	(50)	(0.01)
33% PE	0.35	0.57	8	0.24	140	0.07
	(0.01)	(0.06)	(1)	(0.07)	(50)	(0.01)
50% PE	0.35	0.57	6	0.20	110	0.08
	(0.01)	(0.08)	(1)	(0.06)	(20)	(0.01)

[a] Measurements involved 0.3 mg mL^{-1} SR vesicles in 20 mM MOPS (pH 7.0) at 25 °C. Numbers in parentheses represent the standard deviation from two independent measurements. Analogous errors for individual measurements were obtained from a consideration of the maximal variances obtained from the error surface (*31*), with the exception of ϕ_2 whose maximal variance was approximately 2-fold larger than the indicated values. Parameter values were obtained by fitting the data to eq 4 under Experimental Procedures. [b] Data obtained from reference (*27*).

and the overall rotational motion of the Ca-ATPase with respect to the membrane normal ($\phi_2 \approx 100\ \mu$s; Table 2) (*27*).

PE-Induced Dynamic Structural Changes. The rotational dynamics of the Er-ITC-labeled Ca-ATPase were measured in the presence of varying amounts of PE. Irrespective of the PE concentration, two rotational correlation times and a residual anisotropy are necessary to adequately describe the data (see above). However, upon increasing the PE content in the membrane, the frequency−response values of the differential phase and modulated anisotropy are shifted to higher frequencies (Figure 6), which is indicative of increased rotational mobility. A consideration of the fitting parameters obtained at each PE concentration indicates that the PE-induced increase in the rotational dynamics of the Ca-ATPase primarily results from an increase in the amplitude (g_1) associated with domain motion (ϕ_1); no significant changes in the rotational correlation times or residual anisotropies (r_∞) occur upon altering the PE content of the membrane (Table 2). These rotational correlation times (i.e., ϕ_1 and ϕ_2) are sensitive to changes in the average structure of the phosphorylation domain, alterations in the interaction between Ca-ATPase polypeptide chains, or changes in membrane fluidity (*27*). Likewise, the residual anisotropies are sensitive to differences in the average orientation of the phosphorylation domain relative to the membrane normal (*34*, *35*). Thus, these results indicate that PE does not directly modify the average conformation of the phosphorylation domain, interactions between Ca-ATPase polypeptide chains, or the membrane fluidity. Rather, PE headgroups modulate the dynamic structure of the phosphorylation domain within individual Ca-ATPase polypeptide chains.

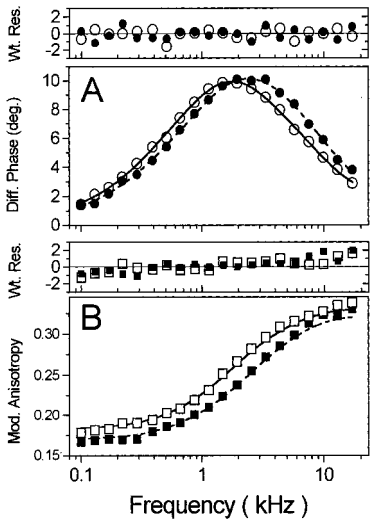

FIGURE 6: Influence of PE on the rotational dynamics of the Ca-ATPase. Differential phase (A; ○,●) and modulated anisotropy (B; □,■) data and corresponding weighted residuals for 0% (○, □) and 50% (mol/mol) (●,■) PE. Lines represent multiexpontial fits for 0% (solid line) and 50% (dotted lines) PE. Experimental conditions are as indicated in the legend to Figure 3.

Measurements of Phospholipid Acyl Chain Structure and Dynamics. The enhancement of the catalytic activity of the Ca-ATPase observed in the presence of PE may be related to differences in structural interactions between membrane phospholipids, which have previously been shown to modulate the catalytic activity of the Ca-ATPase (*36*, *37*). Fluorescence lifetime measurements of the phospholipid analogue TMA-DPH partitioned into binary mixtures of phospholipids containing variable amounts of PE have previously been shown to be sensitive to PE-induced alterations in the average conformation of phospholipid headgroups in binary mixtures of membrane phospholipids (*26*, *38*). We have therefore used frequency-domain spectroscopy of TMA-DPH partitioned into reconstituted prepa-

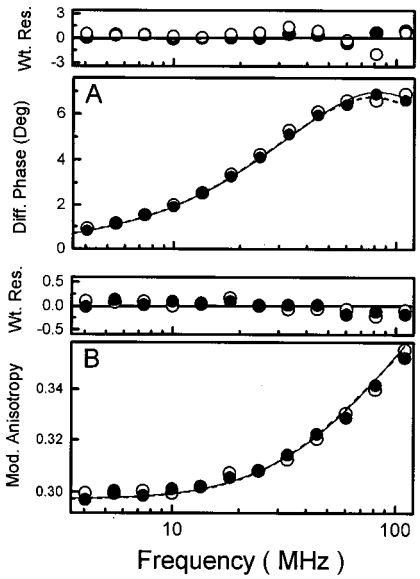

FIGURE 7: Phospholipid acyl chain rotational dynamics. Data and corresponding weighted residuals are shown for TMA-DPH partitioned into reconstituted membranes containing 0% (○) and 50% (●) PE for the differential phase (A) and modulated anisotropy (B). Data were fit as previously described, where $S = (r_\infty/r_o)^{1/2}$ and $r_o = 0.38 \pm 0.02$ (*83*). For 0% PE, $\phi_1 = 2.8 \pm 0.2$ ns and $S = 0.739 \pm 0.003$. For 50% (mol/mol) PE, $\phi_1 = 3.0 \pm 0.2$ ns and $S = 0.743 \pm 0.004$. Experimental conditions are as indicated in the legend to Figure 3.

rations of the Ca-ATPase containing variable amounts of PE to investigate possible differences in the headgroup structure of membrane phospholipids. Two lifetime components are necessary to adequately describe the frequency−response of TMA-DPH (i.e., $f_1 = 0.20 \pm 0.03$; $\tau_1 = 1.2 \pm 0.2$; and $\tau_2 = 4.5 \pm 0.2$), which were found to be essentially independent of the PE content of the bilayer (data not shown). Likewise, the rotational dynamics of TMA-DPH were found to be independent of the PE content of the bilayer (Figure 7), suggesting that PE headgroups do not modulate the functional activity of the Ca-ATPase through alterations in the rotational dynamics of membrane phospholipid acyl chains (i.e., membrane fluidity) or as a result of PE-induced differences in headgroup hydration. These results suggest that PE headgroups may directly interact with the Ca-ATPase through specific electrostatic interactions.

DISCUSSION

Summary of Results. The presence of phospholipids containing phosphoethanolamine headgroups enhances the catalytic activity of the Ca-ATPase (Figure 2), confirming previous suggestions that PE can modulate the catalytic activity of the Ca-ATPase (*8*−*11*). Measurements of the rotational dynamics of Er-ITC bound to Lys_{464} have previously been demonstrated to permit the resolution of the amplitude (g_1) and rate (ϕ_1) of rotational motion of the phosphorylation domain of the Ca-ATPase (*27*). Increases in the amplitude of rotational motion involving the phosphorylation domain of the Ca-ATPase correlate with enzyme activation by PE headgroups (Figure 8). In the presence of increasing amounts of PE, the rotational dynamics of the phosphorylation domain and rates of ATP hydrolysis approach those observed in native membranes (Table 2; Figure 2), which contain 16 ± 4% PE. Thus, DOPE can substitute

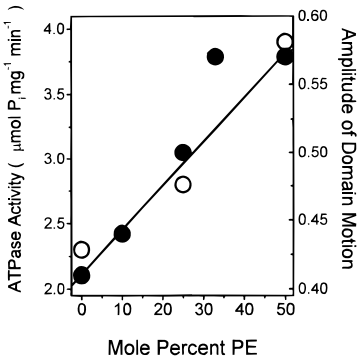

FIGURE 8: Correlation between ATPase activity and rotational dynamics of the phosphorylation domain. Data corresponding to PE-dependent changes in the calcium-dependent ATPase activity (○) or the amplitude of rotational dynamics (g_1) of the phosphorylation domain (●) for Er-ITC-modified Ca-ATPase are replotted from Figure 2 and Table 2, respectively.

for native SR phospholipids that normally function to facilitate dynamic structural changes critical for optimal catalytic function. The PE content of the membrane does not alter the overall protein rotational mobility of the Ca-ATPase or the rotational dynamics of surrounding phospholipid acyl chains (Figure 7, Table 2). Therefore, enhancement of enzymatic activity by PE headgroups is not the result of alterations in the degree of interaction between Ca-ATPase polypeptide chains or differences in acyl chain packing. Rather, specific interactions between PE headgroups and the Ca-ATPase appear to induce internal structural changes within individual Ca-ATPase polypeptide chains that act to optimize catalytic function. These results suggest that the phospholipid environment within SR membranes has an important influence on catalytically important motions, and can modify the structural coupling between the spatially distant high-affinity calcium binding sites located within transmembrane helices and the phosphoester intermediate located at Asp_{351} within the cytoplasmic portion of the phosphorylation domain.

Role for Lipid−Protein Interactions. Early studies have suggested a specific role for the lipids adjacent to membrane proteins in modulating function (*41*−*44*), and that functionally relevant protein−protein interactions are often modulated by weak interaction energies between integral membrane proteins and their associated lipids (*45*−*51*). Furthermore, many hydrophobic drugs (e.g., anesthetics) may act at the lipid−protein interface (*36*, *52*−*54*), emphasizing the possible importance of specific lipid−protein interactions in modulating catalytic activity. The SR Ca-ATPase provides a suitable model to investigate the influence of specific membrane phospholipids and associated differences in bilayer physical properties in the modulation of the catalytic activity of active transport proteins, since its biochemical kinetics are thoroughly documented, structural information is available for different conformational intermediates, and detailed models have been proposed for the mechanism of active transport (*27*, *55*−*58*). Additionally, the maximal catalytic function of the Ca-ATPase has been shown to be dependent on the presence of a fluid bilayer of optimal thickness (*59*−*63*). However, within the context of these structural constraints that are both necessary for catalytically important protein motions and prevent nonspecific protein−protein associations (*63*), the phospholipid headgroup composition

of the bilayer has also been shown to modulate catalytic activity. Thus, anionic phospholipid headgroups inhibit transport function, while phosphoethanolamine headgroups function to maximize catalytic activity and efficient calcium resequestration into native SR membranes (*8*−*11*, *51*, *64*) (Figure 2). Different phospholipid headgroups have similar affinities for the Ca-ATPase and undergo fast exchange on the time-scale of enzyme turnover (*65*), suggesting that there are no strong interactions between membrane phospholipids and the Ca-ATPase that modulate catalytic function. However, phospholipids that undergo fast exchange on the time-scale of enzyme turnover have been shown to retain their essential structural role in modulating enzyme function through the formation of transient hydrogen bonds or alternatively as a result of differences in the lateral tension (elastic stress) within the plane of the bilayer (*4*−*7*, *64*, *66*−*68*).

The mechanisms responsible for the enhanced catalytic function of the Ca-ATPase and other membrane proteins in the presence of PE headgroups have remained unclear, in part, because of an inability to measure catalytically important structural changes involved in calcium translocation. The recent identification of global structural changes involving the spatial rearrangement of major domains in the cytoplasmic portion of the Ca-ATPase upon calcium activation has permitted the current investigation regarding how PE headgroups may modulate conformational transitions important for Ca-ATPase function (*27*, *58*). These recent results are consistent with earlier suggestions that the reorientation of transmembrane helices accompanies calcium activation (*69*). Thus, upon calcium activation, structural changes modify the electron density of the Ca-ATPase in the stalk regions near the membrane surface, resulting in enhanced rotational dynamics of the phosphorylation domain (*27*, *48*). These changes in helical contact interactions within the stalk region may represent the physical basis of the vectorial transport of calcium coupled to ATP hydrolysis, and have been suggested to facilitate the long-range structural coupling between the phosphoester intermediate at Asp_{351} in the cytosolic portion of the phosphorylation domain and the high-affinity calcium binding sites located in the transmembrane helices (*27*, *48*). The observed correlation between maximal enzymatic activity, the mobility of the phosphorylation domain, and the PE content in the membrane provides a strong indication that there are direct interactions between PE headgroups and the Ca-ATPase that facilitate catalytically important motions (Figure 8). Thus, PE headgroups appear to undergo specific interactions with elements of the Ca-ATPase that modify the structural dynamics of the phosphorylation domain. These interactions are not the result of packing defects between phospholipid acyl chains, since PE headgroups do not alter phospholipid acyl chain dynamics or the overall rotational motion of the Ca-ATPase (Figure 7; Table 2).

Physical Significance of PE-Dependent Dynamic Structural Changes of the Ca-ATPase. The recent identification of distinct lobes in the cytosolic portion of the Ca-ATPase whose spatial arrangement changes during the catalytic cycle of the Ca-ATPase offers important clues regarding the mechanism of vectorial calcium transport, which involves the mutual destabilization between high-affinity calcium binding within the transmembrane helices and the formation of the phosphoester intermediate at Asp_{351} in the phosphorylation domain (*27*, *57*, *58*, *70*, *71*). Changes in domain mobility that accompany calcium activation have been suggested to result from differences in the stiffness of the collinear stalk region of the Ca-ATPase located between the transmembrane helices and cytosolic domain, which may result from a reorientation of transmembrane helices associated with calcium binding (see above). Previous results have shown that the Ca-ATPase undergoes uniaxial rotational motion with respect to the membrane normal ($\phi_2 \approx 100\ \mu s$; Table 2), and that the residual anisotropy (r_∞) is related to the orientation of Er-ITC relative to the membrane normal (*27*, *34*, *35*). There is a 20-fold difference between the rates of motion involving the entire Ca-ATPase and the phosphorylation domain ($\phi_2 \approx 6\ \mu s$), indicating that these rotational correlation times represent independent motions (*28*). Therefore, one can obtain an appreciation of the structural changes involving the phosphorylation domain of the Ca-ATPase that alters the preexponential factor (g_1) in the multiexponential decay of anisotropy through a consideration of the relationship between g_1 and the orientational mobility or amplitude of rotational motion. Assuming the motion of the phosphorylation domain has cylindrical symmetry relative to a single flexible hinge, then to a good approximation one can calculate the semiangle (θ_c) of the rotational motion within a cone (*28*, *72*, *73*), where:

$$(1 - g_1) = \left[\frac{1}{2}\cos\theta_c(1 + \cos\theta_c)\right]^2 \qquad (6)$$

Previous results indicate that the semi-angle associated with the amplitude of the rotational motion of the phosphorylation domain of the Ca-ATPase in native SR membranes (i.e., θ_c) is approximately 44°, and increases by about 4° upon calcium activation (*27*). It is therefore of interest to consider the amplitude of rotational motion for the phosphorylation domain in reconstituted preparations containing variable amounts of PE, which progressively increases from a semiangle of 33° in the absence of PE to 42° in the presence of 50% (mol/mol) DOPE (Table 2). There are corresponding increases in the catalytic activity that approach that characteristic of the Ca-ATPase in native SR membranes (Figure 2). Thus, the increased amplitude of motion may facilitate the transfer of the γ-phosphoryl group from ATP bound to the nucleotide binding domain to form the phosphoester linkage at Asp_{351} in the phosphorylation domain.

The exact physical nature of the interaction between phosphoethanolamine headgroups and the Ca-ATPase remains somewhat uncertain. However, the insensitivity of phospholipid acyl chain rotational dynamics (Figure 7) or the overall rotational dynamics of the Ca-ATPase (i.e., ϕ_2) to alterations in the PE content of the bilayer suggests that PE does not alter the lateral tension within the plane of the bilayer, which would be expected to affect the volume available to individual phospholipid acyl chains (*26*). Rather, these results suggest that PE headgroups may modulate Ca-ATPase function through specific intermolecular interactions between phosphoethanolamine headgroups and specific amino acids (e.g., tryptophan) located near the bilayer surface. Consistent with a specific interaction between phosphoethanolamine headgroups and the Ca-ATPase, we find that the average excited-state lifetime of TMA-DPH is

insensitive to changes in the PE content of these reconstituted proteoliposomes. In contrast, previous results obtained for binary mixtures of DOPE and DOPC in unilamellar liposomes indicate that the average lifetime of TMA-DPH increases in proportion to the PE content in the bilayer due to differences in the average conformations of the PE and PC headgroups relative to the bilayer (*26*). Thus, the presence of the Ca-ATPase functions to constrain the orientational freedom of PE headgroups, providing strong evidence of specific interactions between the phosphoethanolamine headgroup and the Ca-ATPase. In this respect, it is worth remembering that tryptophan side chains are commonly observed at the level of the bilayer surface in membrane proteins (including the Ca-ATPase), and have been suggested to function to modulate interhelical interactions and stabilize protein structure through the formation of hydrogen bonds with phospholipid headgroups (*57*, *75*). Thus, given the unique ability of PE headgroups to form strong intermolecular hydrogen bonds within the plane of the bilayer (*76*), differences in the PE content of the bilayer may modulate the structural coupling between the spatially distant calcium binding sites located in the transmembrane helices and the nucleotide binding domain located in the cytoplasmic portion of the Ca-ATPase (*70*, *77*, *78*).

Conclusions and Future Directions. PE headgroups function to facilitate dynamic structural changes involving the phosphorylation domain, which enhances the catalytic function of the Ca-ATPase (Figure 8). There are no significant changes in lipid fluidity or protein−protein interactions between Ca-ATPase polypeptide chains (Figure 7; Table 2), indicating that interactions between the phosphoethanolamine headgroups and the Ca-ATPase play a critical role in maintaining optimal catalytic activity. Future studies should aim to differentiate between specific intermolecular interactions that result from the presence of the quaternary amine in the phosphoethanolamine moiety of PE from functional effects that may arise as a result of differences in headgroup orientation that arise as a result of differences in the size of the phosphoethanolamine and phosphocholine headgroups.

REFERENCES

1. Garrett, K. O., Prence, E. M., and Glew, R. H. (1985) *Arch. Biochem. Biophys. 328*, 344−352.
2. Ganguly, P. K., Rice, K. M., Panagia, V., and Dhalla, N. S. (1984) *Circ. Res. 55*, 504−512.
3. Canty, D. J., and Zeisel, S. H. (1994) *Nutr. Rev. 52*, 327−339.
4. Yeagle, P. L. (1989) *FASEB J. 3*, 1833−1842.
5. Hui, S. W., and Sen, A. (1989) *Proc. Natl. Acad. Sci. U.S.A. 86*, 5825−5829.
6. Gruner, S. M., and Shyamsunder, E. (1991) *Ann. N.Y. Acad. Sci. 625*, 685−697.
7. Kralj-Iglic, V., Svetina, S., and Zeks, B. (1996) *Eur. J. Biophys. (Germany) 24*, 311−321.
8. Hidalgo, C., Petrucci, D. A., and Vergara, C. (1982) *J. Biol. Chem. 257*, 208−216.
9. Navarro, J., Toivio-Kinnucan, M., and Racker, E. (1984) *Biochemistry 23*, 130−135.
10. Cheng, K. H., Lepock, J. R., Hui, S. W., and Yeagle, P. L. (1986) *J. Biol. Chem. 261*, 5081−5087.
11. Gould, G. W., McWhirter, J. M., East, J. M., and Lee, A. G. (1987) *Biochim. Biophys. Acta 904*, 36−44.
12. Huang, S., Negash, S., and Squier, T. C. (1998) *Biochemistry 37*, 6949−6957.
13. Fernandez, J. L., Rosemblatt, M., and Hidalgo, C. (1980) *Biochim. Biophys. Acta 599*, 552−568.
14. Folch, J., Lees, M., and Sloane Stanley, G. H. (1957) *J. Biol. Chem. 226*, 497−509.
15. Hidalgo, C., Ikemoto, N., and Gergely, J. (1976) *J. Biol. Chem. 251*, 224−232.
16. Coll, R. J., and Murphy, A. J. (1984) *J. Biol. Chem. 259*, 14249−14254.
17. Yao, Q., Chen, L. T. L., and Bigelow, D. J. (1998) *Protein Expression Purif. 13*, 191−197.
18. Lévy, D., Gulik, A., Bluzat, A., and Rigaud, J.-L. (1992) *Biochim. Biophys. Acta 1107*, 283−298.
19. Lacapère, J.-J., Stokes, D. L., Olofsson, A., and Rigaud, J.-L. (1998) *Biophys. J. 75*, 1319−1329.
20. Schaffner, W., and Weissman, C. (1973) *Anal. Biochem. 56*, 502−514.
21. Chen, P. S., Toribara, T. Y., and Warner, H. (1956) *Anal. Chem. 28*, 1756−1758.
22. Lanzetta, P. A., Alverez, L. J., Reinsch, P. S., and Candia, O. (1979) *Anal. Biochem. 100*, 95−97.
23. Hunter, G. W. (1997) Doctoral dissertation, p 38, The University of Kansas, Lawrence, KS.
24. Pedigo, S., and Shea, M. (1995) *Biochemistry 34*, 1179−1196.
25. Nicoli, D. F., McKenzie, D. C., and Wu, J.-S. (1991) *Am. Lab. 23*, 32−40.
26. Hunter, G. W., and Squier, T. C. (1998) *Biochim. Biophys. Acta 1415*, 63−76.
27. Huang, S., and Squier, T. C. (1998) *Biochemistry 37*, 18064−18073.
28. Eads, T. M., Thomas, D. D., and Austin, R. H. (1984) *J. Mol. Biol. 179*, 55−81.
29. Weber, G. (1981) *J. Phys. Chem. 85*, 949−953.
30. Lakowicz, J. R., Cherek, H., Maliwal, B. P., and Gratton, E. (1985) *Biochemistry 24*, 376−383.
31. Beechem, J. M., Gratton, E., Ameloot, M., Knutson, J. R., and Brand, L. (1991) *Topics in Fluorescence Spectroscopy* (Lakowicz, J. R., Ed.) Vol. 2, pp 241−306, Plenum Press, New York.
32. Johnson, M. L., and Faunt, L. M. (1992) *Methods Enzymol. 210*, 1−37.
33. Bishop, J. E., Squier, T. C., Bigelow, D. J., and Inesi, G. (1988) *Biochemistry 27*, 5233−5240.
34. Fajer, P., Knowles, F., and Marsh, D. (1989) *Biochemistry 28*, 5634−5643.
35. Cherry, R. J. (1992) in *The Structure of Biological Membranes* (Yeagle, P., Ed.) pp 507−537, CRC Press, Boca Raton, FL.
36. Bigelow, D. J., and Thomas, D. D. (1987) *J. Biol. Chem. 262*, 13449−13456.
37. Squier, T. C., Hughes, S. E., and Thomas, D. D. (1988) *J. Biol. Chem. 263*, 9162−9170.
38. Talbot, W. A., Zheng, L. X., and Lentz, B. R. (1997) *Biochemistry 36*, 5827−5836.
39. Meissner, G., and Fleischer, S. (1971) *Biochim. Biophys. Acta 241*, 356−378.
40. Bigelow, D. J., Squier, T. C., and Thomas, D. D. (1986) *Biochemistry 25*, 194−202.
41. Jost, P. C., Griffith, O. H., Capaldi, R. A., and Vanderkoii, G. A. (1973) *Proc. Natl. Acad. Sci. U.S.A. 70*, 480−484.
42. Jost, P. C., Griffith, O. H., Capaldi, R. A., and Vanderkoii, G. A. (1973) *Biochim. Biophys. Acta 311*, 141−152.
43. Thomas, D. D., Bigelow, D. J., Squier, T. C., and Hidalgo, C. (1982) *Biophys. J. 37*, 217−225.
44. Marsh, D. (1985) in *Progress in Protein−Lipid Interactions* (Watt, A., and DePont, J. J. H. H., Eds.) Vol. 1, pp 143−172, Elsevier Science Publishers, Amsterdam.
45. Owicki, J. C., Springgate, M. W., and McConnell, H. M. (1978) *Proc. Natl. Acad. Sci. U.S.A. 75*, 1616−1619.
46. Owicki, J. C., and McConnell, H. M. (1979) *Proc. Natl. Acad. Sci. U.S.A. 76*, 4750−4754.
47. Pearson, L. T., Edelman, J., and Chan, S. I. (1984) *Biophys. J. 45*, 863−871.
48. Brown, M. F. (1994) *Chem. Phys. Lipids 73*, 159−180.
49. Bogdanov, M., and Dowhan, W. (1995) *J. Biol. Chem. 270*, 732−739.

50. Stubbs, C. D., and Slater, S. J. (1996) *Chem. Phys. Lipids 81*, 185−195.
51. Dalton, K. A., East, J. M., Mall, S., Oliver, S., Starling, A. P., and Lee, A. G. (1998) *Biochem. J. 329*, 637−646.
52. Franks, N. P., and Lieb, W. R. (1987) *Nature 328*, 113−114.
53. Evers, A. S., Berkowicz, B. A., and d'Avignon, D. A. (1987) *Nature 328*, 157−160.
54. Barrantes, F. J. (1993) *FASEB J. 7*, 1460−1467.
55. Inesi, G. (1985) *Annu. Rev. Physiol. 47*, 573−601.
56. Jencks, W. P. (1989) *J. Biol. Chem. 264*, 18855−18858.
57. MacLennan, D. H., Rice, W. J., and Green, N. M. (1997) *J. Biol. Chem. 272*, 28815−28818.
58. Ogawa, H., Stokes, D. L., Sasabe, H., and Toyoshima, C. (1998) *Biophys. J. 75*, 51−52.
59. Lewis, B. A., and Engelman, D. M. (1983) *J. Mol. Biol. 166*, 211−217.
60. Hidalgo, C. (1987) *Crit. Rev. Biochem. 21*, 319−347.
61. Squier, T. C., Bigelow, D. J., and Thomas, D. D. (1988) *J. Biol. Chem. 263*, 9178−9186.
62. Matthews, P. L., Bartlett, E., Ananthanarayanan, V. S., and Keough, K. M. (1993) *Biochem. Cell Biol. (Canada) 71*, 381−389.
63. Cornea, R. L., and Thomas, D. D. (1994) *Biochemistry 33*, 2912−2920.
64. Gruner, S. M. (1989) *J. Phys. Chem. 93*, 7562−7570.
65. London, E., and Feigenson, G. W. (1981) *Biochemistry 20*, 1939−1948.
66. Gruner, S. M. (1985) *Proc. Natl. Acad. Sci. U.S.A. 82*, 3665−3669.
67. Gruner, S. M., Cullis, P., Hope, M. J., and Tilcock, C. P. S. (1985) *Annu. Rev. Biophys. Biophys. Chem. 14*, 211−238.
68. Klein, K., Rudy, B., McIntyre, J. O., Fleisher, S., and Trommer, W. E. (1996) *Biochemistry 35*, 3044−3049.
69. Gryczynski, I., Wiczk, W., Inesi, G., Squier, T. C., and Lakowicz, J. R. (1989) *Biochemistry 28*, 3490−3498.
70. Clarke, D. M., Loo, T. W., Inesi, G., and MacLennan, D. H. (1989) *Nature 339*, 476−478.
71. Inesi, G., Zhang, Z., Sagara, Y., and Kirtley, M. (1994) *Biophys. Chem*. 50, 129−138.
72. Kinosita, K. J., Kawato, S., and Ikegami, A. (1977) *Biophys. J. 20*, 289−305.
73. Kinosita, K., Jr., Ishiwata, S., Yoshimura, H., Asai, H., and Ikegami, A. (1984) *Biochemistry 23*, 5963−5975.
74. Seelig, J., Macdonald, P. M., and Scherer, P. G. (1987) *Biochemistry 26*, 7535−7541.
75. Schiffer, M., Chang, C.-H., and Stevens, F. J. (1992) *Protein Eng. (London) 5*, 213−214.
76. Watts, A., and van Gorkom, L. C. M. (1992) in *The Structure of Biological Membranes* (Yeagle, P., Ed.) pp 307−336, CRC Press, Boca Raton, FL.
77. Squier, T. C., Bigelow, D. J., Fernandez-Belda, F. J., de Meis, L., and Inesi, G. (1990) *J. Biol. Chem. 265*, 13713−13720.
78. Yonekura, K., Stokes, D., Sasabe, H., and Toyoshima, C. (1997) *Biophys. J. 72*, 997−1005.
79. Barrabin, H. M., Scofano, H. M., and Inesi, G. (1984) *Biochemistry 23*, 1542−1548.
80. Bevington, P. R. (1969) *Data Reduction and Error Analysis for the Physical Sciences*, McGraw-Hill, New York.
81. Laemmli, U. K. (1970) *Nature 227*, 680−685.
82. Negash, S., Chen, L. T., Bigelow, D. J., and Squier, T. C. (1996) *Biochemistry 35*, 11247−11259.
83. Squier, T. C., Mahaney, J. E., Yin, J. J., Lai, C. S., and Lakowicz, J. R. (1991) *Biophys. J. 59*, 654−669.

BI9822224